

Rheological Properties of Melt-Compounded Nanocomposites of Atomic-Layer-Deposition-Coated Polyamide and Polystyrene Powders

Katja Nevalainen¹, Reija Suihkonen¹, Tony McNally², Eileen Harkin-Jones²,
Seppo Syrjäälä¹, Jyrki Vuorinen¹, Pentti Järvelä¹, and Nora Isomäki³

¹ Tampere University of Technology, Tampere, Finland

² Queen's University Belfast, Belfast, UK

³ Beneq Oy, Espoo, Finland

ABSTRACT

Polyamide and polystyrene particles were coated with titanium dioxide films by atomic layer deposition and then melt-compounded to form novel polymer nanocomposites. The rheological properties of the materials, characterized with melt flow indexer, melt flow spiral mould, and rotational rheometer, are discussed. Finally, the effect of molecular weight distribution on the observed changes in the properties of the polymers is highlighted.

INTRODUCTION

A novel approach to fabricate highly dispersed polymer nanocomposites is to coat polymer particles with ultra-thin, inorganic films and then melt-compound the coated polymer particles. In extrusion, high shear forces break the ceramic shells of polymer particles and disperse shell remnants throughout the polymer matrix. This method is attractive in terms of, e.g., enhanced nanofiller dispersion¹⁻⁴, improved barrier properties⁵, and easier melt-processing^{4,6}.

A well-tried method for depositing various oxide materials on polymeric particles or film substrates is atomic layer deposition (ALD)^{8,9}, which is a multi-step gas phase adsorption technique analogous to the one-step chemical vapor deposition (CVD) reaction. ALD allows fabrication of precision thickness films with angstrom-

level control.^{7,10} It has been demonstrated that conformal, pinhole-free films can be deposited on the surfaces of nano- and micrometer-sized particles without agglomeration in processing^{1,7,11}. An additional benefit of ALD is that several thin films, e.g., alumina, titanium dioxide, and tungsten, can be deposited at relatively low temperatures (<150°C), thereby reducing, if not altogether eliminating, thermal damage to temperature-sensitive polymers^{1,8,9}.

This paper explores the ALD of polyamide and polystyrene particles. The target was to examine changes in the melt flow behaviour, viscosity, and molecular weight of ALD-created titanium dioxide nanocomposites and understand the reasons behind the marked drop in viscosity observed in our previous work^{4,6}.

EXPERIMENTAL

Materials used

The polymeric powders used were polyamide PA 2200 and polystyrene PS 80/03 with an average particle size of 60 μm ¹² and 80 μm ¹³, respectively, both supplied by EOS GmbH. Nanometer-scale thin films of titanium dioxide (TiO₂) with an approximate nominal thickness of 5, 10, 25, or 40 nm were laid on polyamide (PA) and polystyrene (PS) particles in a commercial ALD reactor (P400, Beneq Oy). The ALD coating process is described elsewhere^{4,6}.

Melt compounding

ALD-coated raw materials were oven-dried at 80°C for several hours. The nanocomposites were melt-compounded in a 5-cm³ DSM microextruder, operating at 200 rpm with 1-minute dwell time. The barrel temperature was 220°C and 190°C, for PA and PS respectively. The specimens were then injection-moulded using a 5-cm³ DSM injection moulding machine, operating at an injection pressure of 50 MPa. For the PA matrix, a barrel temperature of 220°C and a mould temperature of 80°C were used, whereas for PS the corresponding temperatures were 190°C and 30°C, respectively.

Specimen characterization

The amount of inorganic filler in the polymer nanocomposites was determined by an ash content test. Samples of 1–1.5 g were held in an oven with the temperature increasing gradually from 300 to 600 °C over two hours. Their inorganic material weight percentage was computed from the ash weight after burning, divided by the original sample weight.

The melt-mass flow rate (MFR) of the studied polyamide powders was measured according to SFS ISO 1133 on a CEAST melt flow indexer, model 6452/000, at 191°C under a static load of 2.16 kg.

A melt flow spiral test was run by injecting the polymer nanocomposite mixtures into a spiral mould⁶. The flow length was determined as the average flow length of at least six moulded samples of each material studied.

Rheological measurements were carried out with a rotational rheometer (Physica MCR 301). Rotational rheometer experiments were run in parallel-plate geometry, using injection moulded, coin-shaped samples (Ø 25 mm, thickness 1.5 mm). All samples were dried in a vacuum oven for more than 13 hours before testing them under a continuous nitrogen purge to prevent moisture-induced and oxidative degradation of polymers. First, to examine

the thermal stability of the materials, time sweep tests were run under oscillatory shearing at a strain amplitude of 1%, an angular frequency of 10 rad/s, and a gap thickness of 0.5 mm. Second, steady shear experiments were run at two gap settings of 0.5 and 1 mm with shear rates ranging from 0.1 to 10 1/s. Rheological measurements were conducted at 200 °C for PA and at 190 °C for PS matrixes.

Gel permeation chromatography (GPC) was performed on the PS samples with tetrahydrofuran (with antioxidant) as solvent. A solution was prepared by adding 10 ml of solvent to 20 mg of sample. Solutions were then left for 4 hours to dissolve and were thoroughly mixed before being filtered through a 0.2-µm PA membrane. The samples appeared fully dissolved, and the solutions were easy to filter. Chromatograms were obtained using a light scattering, differential pressure, refractive index detector, equipped with a PLgel guard plus 2 x mixed bed-B, 30-cm, 10-µm columns at a flow rate of 1.0 ml/min and a nominal temperature of 30°C. Both solutions were tested in triplicate. The GPC system was calibrated with Polymer Laboratories polystyrene calibrants.

GPC was performed on the PA samples using 1,1,1,3,3,3-hexafluoro-2-propanol (HFIP) as solvent. Solutions were prepared by adding 10 ml of eluent to 20 mg of sample. The solution was left for a minimum of 4 hours to dissolve and then thoroughly mixed and filtered through a 0.45-µm PTFE membrane directly into auto-sampler vials. The dissolved samples were turbid yet easy to filter. Chromatograms were obtained using a refractive index detector, equipped with a PL HFIPgel guard plus 2 x PL HFIPgel 300 x 7.7-mm, 9-µm columns at a flow rate of 0.8 ml/min and a nominal temperature of 40°C. Duplicates of each sample were tested. Our GPC system was calibrated with poly(methyl methacrylate), and the results were expressed in "PMMA-equivalent" molecular weights, suitable for comparative purposes.

RESULTS

Filler content and melt-flow properties

The prepared composites were measured for their ash content. Results indicate that both pure PA and pure PS contained 1.5 wt. % and 0.6 wt.% of some unknown inorganic material, respectively. Because in our previous work we detected impurities in PA by SEM³, we also now, to estimate the nano-TiO₂ content of the polymer matrix, deducted the inorganic impurity material from the nanocomposite's inorganic material content. Results (Fig. 1) show that in the PS matrix, the TiO₂ content increased linearly as a function of the desired ALD-coating thickness.

Due to the smaller particle size of PA^{12,13}, we expected the TiO₂ content of the ALD-coated PA to be higher than that of the ALD-coated PS. However, this occurred (Fig. 1) only with specimens with thicker ALD-coatings (>10 nm). On PA powder, a thin film forms unpredictably with great differences from batch to batch. In our previous work³, e.g., the TiO₂ content of the PA 40-nm ALD was as high as 5.3 wt.%, whereas now the same process settings yielded only 1.1 wt.% of TiO₂. The polymer powder layer in the reaction chamber may have been somewhat thicker in the batch this time to yield a lower TiO₂ content.

The melt-mass flow rate (MFR) was measured to approximate the rheological properties of the studied polymer powders before melt-compounding. The PA powder shows (Fig. 2a) an MFR of 3 g/10 min for unfilled polymer but 200-400% higher values for ALD-created nanocomposites. A similar drastic increase in the MFR and thus a reduction in viscosity were reported also in our previous paper⁶. To study if the drop in viscosity depended on the polymer matrix, we determined the MFR of the ALD-created PS composites. They showed a moderate increase in MFR, yielding only 10-40% higher values than pure PS. However, the results were encouraging and suggested that also in PS nanocomposites viscosity can be decreased at very thin ALD TiO₂ coatings.

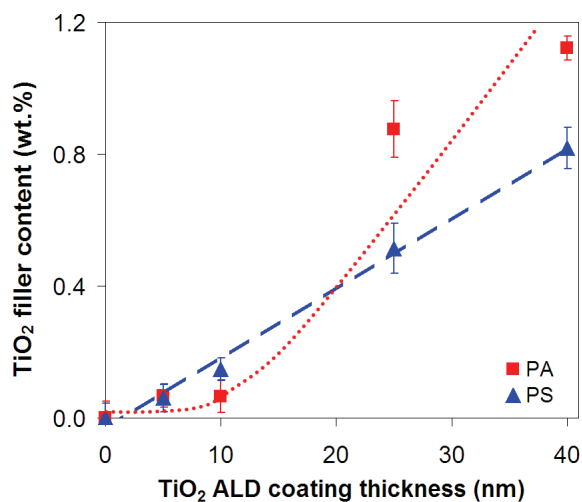


Figure 1. TiO₂ filler content as a function of TiO₂ ALD coating thickness.

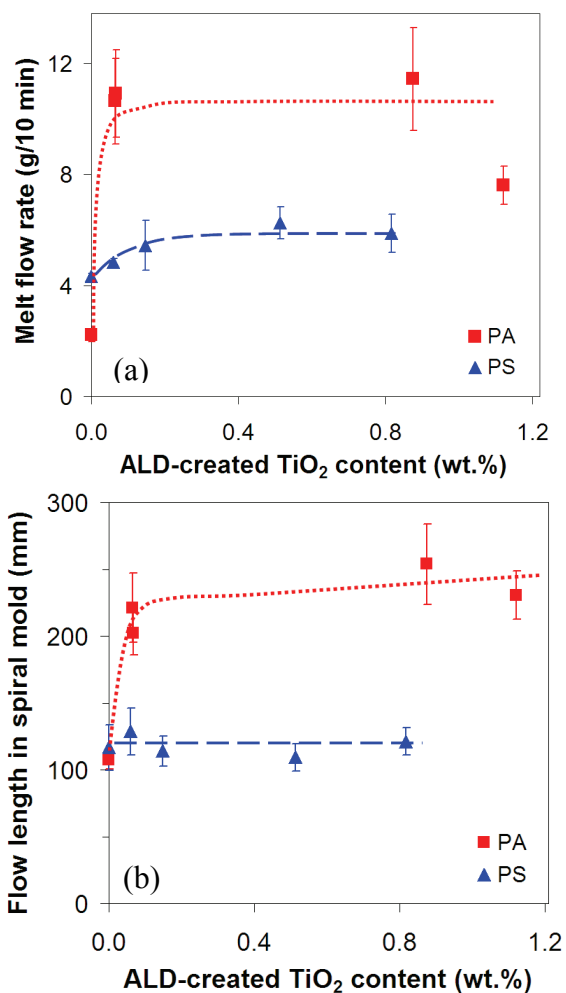


Figure 2. (a) Melt flow rates of ALD-coated polymer powders and (b) flow length of spiral mold for extruded polymer nano-composites as a function of ALD-created TiO₂ content.

To confirm the MFR results, we used a spiral mould tool to compare relatively the final flow length of the melt-compounded nanocomposites. Spiral flow results (Fig. 2b) show that the ALD-created PA nanocomposites possess a significantly longer spiral length than pure PA. This change was observed already at low ALD-coating thicknesses, as MFR values suggested. Unexpectedly, no such drop in viscosity was observed in PS nanocomposites. Why changes in PS viscosity were not detected in the spiral mould test but rather in the MFR test could be because of the stronger shear-thinning of PS over PA (Fig. 4).

Since temperature and shear-rate remained virtually constant in the MFR test, the drop in the viscosity of the nanocomposites may be traced to two factors: (1) flow improvement by ALD-created TiO₂ due to a wall slippage and a polymer chain slipping over TiO₂ fillers and/or (2) reduction in molecular weight following the degradation and chain scission of the polymer matrix during melt-compounding, as suggested for polyamide nanocomposites by other authors^{14,15}. Our previous studies^{4,6} of ALD-coated PA nanocomposites suggest no significant thermal degradation, as demonstrated by similar viscoelastic and thermal behaviour between ALD-created nanocomposites and pure PA. The following discusses experiments on thermal stability and a possible bulk property such as the lubricating/plasticizing effect of ALD-created TiO₂ and/or the wall slip phenomenon.

Viscosity and wall slip

Before steady shear viscosity measurements, the thermal stability of the materials was evaluated in the oscillatory shear mode by monitoring the complex viscosity as a function of time (Fig. 3). Apparently, no significant degradation occurred in the specimens' polymer chain during the 30-min. test, as indicated by the

constant or even increased complex viscosity values for PS and PA, respectively. Such time-dependent complex viscosity behaviour of PA has been reported also by others and can be explained by a postcondensation reaction of the material that increases the molecular weight¹⁶.

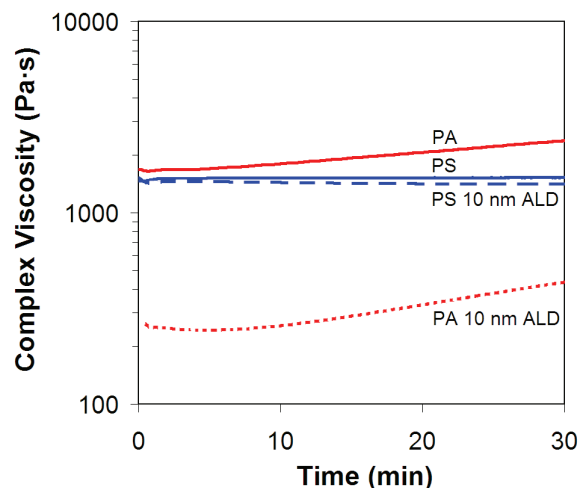


Figure 3. Complex viscosity as a function of time for PA and PS TiO₂ nanocomposites measured at 200°C and 190°C, respectively.

The value in the branches is the gap distance.

The decrease in viscosity of ALD-created PA nanocomposites, observed also in previous studies^{4,6}, is now considered to be a bulk property and/or related to surface effects such as a wall slip. In wall slip, the melt flows by slipping along the walls of the moulding system without sticking. Wall slip occurs generally due to the formation of a lubricated layer along the wall. The most common is an apparent wall slip owing to, e.g., particle migration (generally away from this region or a higher concentration of lower molecular weight species near the wall) and alignment of polymer molecules. The wall slip of entangled molten polymers is a surface-to-volume-dependent phenomenon^{17,18}. Therefore, steady shear experiments were run with two different gap sizes. During a wall slip, the smaller gap (where material plate contact dominates over material property) should yield lower viscosity values.

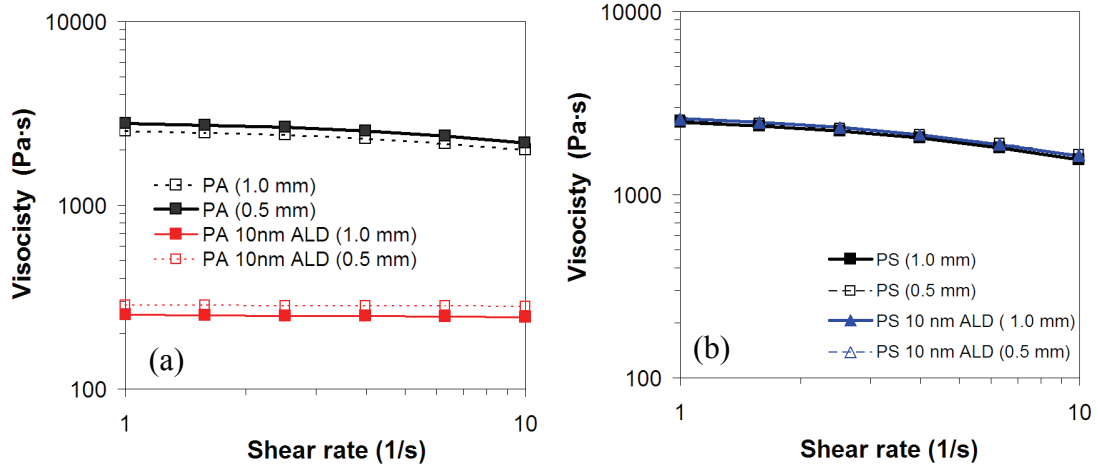


Figure 4. Viscosity as a function of shear rate for (a) PA and (b) PS TiO₂ nanocomposites, measured at 200°C and 190°C, respectively. The value in the branches is the gap distance.

The shear viscosity results given as a function of shear rate (Fig. 4) for the ALD-created composites and reference matrixes demonstrate that the decrease in viscosity is evident only for the polyamide nanocomposites. The viscosity of PS remains unchanged after ALD-nanocomposite formation, as the spiral melt flow results suggested. Furthermore, within experimental uncertainty, the variation in gap size has no significant effect on the viscosity. Consequently, the results imply that the ALD-created decrease in viscosity is a material-dependent property and not a mere near wall phenomenon.

Molecular weight distribution

Rheological properties of entangled polymer melts depend strongly on the polymer molecular weight, because molecular relaxation times increase rapidly with increasing molecular weight. It has been proposed that¹⁹

$$\eta_0 = M_w^{3.4} \quad (1)$$

where M_w is the weight-average molecular weight of the polymer (kg/kgmol) and η_0 the intrinsic viscosity of the polymer. If a relationship develops between two

molecular weights M_{w_1} and M_{w_2} of a material with different zero-shear-rate viscosities, then the following equation applies:

$$\frac{M_{w_1}}{M_{w_2}} \sim \left(\frac{\eta_{0_1}}{\eta_{0_2}} \right)^{\frac{1}{3.4}} \quad (2)$$

where η_{0_1} and η_{0_2} are the corresponding viscosity values. If the values of $\eta_{0_1} = 2430 \text{ Pa} \cdot \text{s}$ for extruded PA and $\eta_{0_2} = 238 \text{ Pa} \cdot \text{s}$ for extruded PA 10 nm ALD (values taken from Fig. 4a at a shear rate of 1/s) are used in Eq. 2, then $M_{w_2} \sim 0.5M_{w_1}$. The result suggests that the molecular weight of the ALD-created PA nanocomposite decreases by 50% due to the ALD-coated material, if the reduction of molecular weight in the material is the only mechanism causing low viscosity.

GPC measurements were run to confirm the above statement. Results (Table 1) show that the average molecular weights (M_n and M_w) and the polydispersity index (PDI) of PS were not affected by the presence of ALD-created TiO₂ nanoparticles. However, contrary to our previous conclusions drawn from thermal studies^{4,6}, the molecular

weight of the PA ALD nanocomposites decreased significantly, in fact, by about 50%, which agrees well with the calculated value.

Table 1. GPC results of extruded PA and PS TiO₂ nanocomposites.

Material	M _w ^a (10 ³ g/mol)	M _n ^a (10 ³ g/mol)	PDI
PA	34	9.4	3.6
PA 10 nm ALD	17	4.4	3.9
PS	129	37	3.5
PS 10 nm ALD	131	38	3.4

^a Standard deviation values were ±0.3 and ±2 for PA and PS, respectively.

Because the molecular weight of the polymer drops uncontrollably and depends on the material, the phenomenon is considered an undesired property change. Concern over the terms of the molecular degradation of polymers first arose after the compositional data of the ALD film on the PA⁴ and PS particles had been tested with an energy dispersive spectrometer. Results suggested that the thin film contained a significant amount of chlorine (0-14 wt.%). Clearly, if purging is not effective enough during ALD-coating, some precursor remnants and byproducts of chemical reactions may remain in the coated material. Generally, the amount of impurities in the resulting film depends on the substrate temperature, which is often higher at low processing temperatures²⁰. The precursors we used in ALD-coating^{3,4}, titanium tetrachloride (TiCl₄) and water (H₂O), create hydrochloric acid (HCl) as a byproduct in TiO₂ thin-film formation. PA resists poorly strong acids such as HCl, whereas PS may withstand HCl somewhat better²¹. This difference in their chemical resistance may be one reason for the different degradation behavior of the studied polymers. Furthermore, the combination of moisture and photoactive TiO₂ may lead to uncontrollable polymer degradation, especially with PA.

CONCLUSIONS

The significantly lower viscosity of the ALD-created TiO₂ polyamide nanocomposite originated from the molecular degradation of the polymer, whereas no such behavior was observed in the PS ALD nanocomposites. Apparently, the resistance of the PS matrix against humidity, precursor remnants, and byproducts (such as HCl) and reactive TiO₂ is higher than that of PA, especially at elevated processing temperatures. Consequently, the optimization of the chemical composition of ALD-created coating in polymeric nanocomposites requires further study. Research is required to minimize especially chlorine residues left from ALD coating. In addition, it would be fascinating to examine the effects of more stable sandwich structures such as Al₂O₃/TiO₂/Al₂O₃ ALD-created nanofillers on the properties of PA and PS.

ACKNOWLEDGMENTS

The financial support from the Finnish Funding Agency for Technology and Innovation and The Graduate School of the Processing of Polymers and Polymer-Based Multimaterials is gratefully acknowledged. Dr. Steve Holding and Smithers Rapra are also acknowledged for their assistance with GPC analysis.

REFERENCES

1. Spencer, J.A., Liang, X., George, S.M., Buechler, K.J., Blackson, J., Wood, C.J., Dorgan, J.R., and Weimer, A.W. (2007), "Fluidized bed polymer particle ALD process for producing HDPE/Alumina nanocomposites", *12th Int. Conf. Fluidiz.-New Horizons Fluidiz. Eng.*, **RP4**, 417-424.
2. Liang, X., Hakim, L.F., Zhan, G.-D., McCormick, J.A., George, S.M., Weimer, A.W., Spencer, J.A., Buechler, K.J., Blackson, J., Wood, C.J., and Dorgan J.R. (2007), "Novel processing to produce polymer / ceramic nanocomposites by

- atomic layer deposition”, *J. Am. Ceram. Soc.*, **90**, 57-63.
3. Nevalainen, K., Suihkonen, R., Eteläaho, P., Vuorinen, J., Järvelä, P., Isomäki, N., Hintze, C., and Leskelä, M. (2009), “Mechanical and tribological property comparison of melt-compounded nanocomposites of atomic-layer-deposition-coated polyamide particles and commercial nanofillers”, *J. Vac. Sci. Technol. A*, **27**, in press.
 4. Nevalainen, K., Hintze, C., Suihkonen, R., Sundelin, J., Eteläaho, P., Vuorinen, J., Järvelä, P., and Isomäki, N. (2008), “Thermal and rheological behaviour comparison of melt compounded nanocomposites of atomic-layer-deposition-coated polyamide particles and commercial nanofillers”, *J. Nanostruct. Polym. Nanocomp.*, **4**, 128-138.
 5. Liang, X., King, F.M., Groner, M.D., Blackson, J.H., Harris, J.D., George, S.M., and Weimer, A.W. (2008), “Barrier properties of polymer/alumina nanocomposite membranes fabricated by atomic layer deposition”, *J. Membr. Sci.*, **322**, 105-112.
 6. Nevalainen, K., Hintze, C., Suihkonen, R., Eteläaho, P., Vuorinen, J., Järvelä, P., and Isomäki, N. (2008), “Rheological properties of melt-compounded and diluted nanocomposites of atomic-layer-deposition-coated polyamide particles”, *Ann. Trans. Nordic Rheol. Soc.*, **16**, 125-133.
 7. King, D.M., Liang, X., Li, P., and Weimer, A.W. (2008), “Low-temperature atomic layer deposition of ZnO films on particles in a fluidized bed reactor”, *Thin Solid Films*, **516**, 8517–8523.
 8. Kemell, M., Färm, E., Ritala, M., Leskelä, M. (2008), “Surface modification of thermoplastics by atomic layer deposition of Al₂O₃ and TiO₂ thin films”, *Eur. Polym. J.*, **44**, 3564–3570.
 9. Wilson, C.A., McCormick, J.A., Cavanagh, A.S., Goldstein, D.N., Weimer, A.W., and George, S.M. (2008), “Tungsten atomic layer deposition on polymers”, *Thin Solid Films*, **516**, 6175.
 10. Ritala, M. and Leskelä, M. (1999), “Atomic layer epitaxy – a valuable tool for nanotechnology”, *Nanotechnology*, **10**, 19-24.
 11. Hakim, F., Blackson, J., George, S.M., and Weimer A.W. (2005), “Nanocoating individual silica nanoparticles by atomic layer deposition in a fluidized bed reactor”, *Chem. Vap. Deposition*, **11**, 420-425.
 12. EOS GmbH. (2001), “Produktinformation EOSINT P / PA2200-Pulver”, *Data Sheet* (in German), 12 p.
 13. Keller, P. from EOS GmbH (2008), Personal communication.
 14. McNally, T., Murphy, W. R., Lew, C.Y., Turner, R.J., and Brennan, G.P. (2003), “Polyamide-12 layered silicate nanocomposites by melt blending”, *Polymer*, **44**, 2761-2772.
 15. Xu, G., Chen, G. Ma, Y., Ke, Y., and Han, M. (2008), “Rheology of a low-filled polyamide 6/montmorillonite nanocomposite”, *J. Appl. Polym. Sci.*, **108**, 1501-1505.
 16. Acierno, S. and Puyvelde P. Van (2005), “Rheological behavior of polyamide 11 with varying initial moisture content”, *J. Appl. Polym. Sci.*, **97**, 666-670.
 17. Xu, J., Costeux, S., Dealy, J.M., and Decker, M.N.D. (2007), “Use of a sliding plate rheometer to measure the first normal stress difference at high shear rates”, *Rheol. Acta*, **46**, 815–824.

18. Rides, M., Allen, C., Fleming, D., Haworth, B., and Kelly, A. (2008), "Intercomparison of slip flow velocity measurements of filled polymers by capillary extrusion rheometry", *Polym. Testing*, **27**, 308–320.
19. Kemplowski, Z. and Torzecki, J. (1983) "Determination of the weight-average molecular weight of polyamide-6 on the basis of melt viscosity", *Rheol. Acta*, **22**, 186-196.
20. Jogi, I. (2007), Conduction Mechanisms in Thin Atomic Layer Deposited Films Containing TiO₂. Dissertation, University of Tartu, Estonia. pp. 124.
21. LATI, High performance thermoplastics "Chemical resistance data", **Ed. 03/02**, (www.lati.com/pdf/technical_data/chemical_resistance.pdf), pp. 8.